Multi-Element Fully-Decoupled Inverted-F Antennas for Mobile Terminals

Jiangwei Sui, *Member, IEEE,* Cuixia Huang, and Yi-Feng Cheng, *Member, IEEE*

***Abstract*—In this paper, a multi-element fully-decoupled linearly-placed inverted-F antenna (IFA) array is proposed for mobile terminals. A hybrid decoupling method is used to mitigate the mixed types of mutual couplings among the multiple IFAs: introducing multiple decoupling capacitors for the couplings of two back-to-back IFA pairs and T-shaped mode transformers for the remaining couplings. The decoupling capacitors not only decouple the back-to-back IFA pairs but also broaden the impedance bandwidth of each IFA. The T-shaped mode transformer transforms the concerned antenna from an IFA mode into a balanced loop mode, preventing the induced current on the victim IFAs of the face-to-face and back-to-face pairs. One four-element example and one eight-element example are designed and measured to justify the proposed decoupling concept. The measured results of the four-element IFAs show that after decoupling, all the six mutual couplings among the four IFAs are reduced by about 10 dB from 3.3 to 3.8 GHz, with average total efficiencies throughout the band improving from 57 % to 72 % for IFA 1 and from 47 % to 55 % for IFA 2. An eight-element IFA array is built utilizing the pattern diversity of two proposed four-element IFA blocks, achieving inter-block isolation of better than 20 dB. And a six-element linear IFA array is also designed to prove the generality of the proposed method.**

***Index Terms*—Antenna decoupling, inverted-F antenna (IFA), mobile terminals, multi-element, multi-input and multi-output (MIMO), mutual coupling.**

I. Introduction

According to Shannon's theorem, to have a higher data rate, more antennas and wider bands can be adopted. For more antennas, multi-input and multi-output (MIMO) antennas have been widely used in wireless terminals to deliver different data streams simultaneously on the same carrier band. To provide more frequency resources for 5G communications, a 3.5 GHz band, N78, was allocated as a 5G band in 2015 [1]. Since then, how to integrate high-order MIMO antennas (antenna number ≥ 4) of the N78 band into mobile terminals has drawn great attention from industry and academia. However, due to the volume limitation in mobile terminals, when the antenna number increases, there will inevitably generate mutual couplings among antenna elements, which severely degrades the MIMO systems' performance [2], [3].

In the past decades, to solve the mutual coupling problems in mobile terminals, various decoupling methods have been proposed, such as the use of neutralization lines [4], [5], decoupling circuits [6], [7], characteristic modes [8], [9], parasitic elements [10], [11], decoupling branches [12], filtering slots [13], and decoupling capacitors [14], just name a few. The core mechanism behind these decoupling methods is cancellation, such as admittance cancellation [4] – [7], mode cancellation [8], [9], and coupling cancellation [10] – [14], and a distinctive feature is that there is a transmission zero of the transmission coefficient S_{21}, also called decoupling notch, within the desired band. However, these methods mainly focus on the mutual coupling problems of two antennas.

Very recently, many efforts have been devoted to the coupling reduction of high-order MIMO antennas. One straightforward method is utilizing the polarization and spatial diversity of the MIMO antennas [15], [16]. Another effective method is designing a two-element decoupled antenna pair as a basic block, and then using two or more blocks to form a high-order MIMO antenna system [17] – [23]. In [17], two asymmetrically mirrored gap-coupled loop antennas form the basic building block for eight-antenna MIMO design, achieving inherent isolation between the two antennas in 3.4 – 3.6 GHz. In [18], a two-element antenna pair is self-decoupled by sharing the same grounding branch, and two such pairs are used to form a four-element MIMO antenna system. Besides, the orthogonal modes methods are recently widely studied by skillfully exciting the common and differential modes to achieve a self-decoupled antenna pair. These pairs can be a bent monopole and an edge-fed dipole [19], a T-shaped monopole and a balun-fed dipole [20], a cable-fed in-phase mode antenna and a slot mode antenna [21], a T-shaped monopole antenna and a cable-fed T-shaped slot antenna [22], and a balun-fed dipole/slot mode antenna and a monopole/slot mode antenna [23]. Although these methods can achieve high isolation within the two antennas of the pair, they do not decouple the antennas belonging to different pairs, usually separating two pairs as far as possible to reduce the inter-pair mutual coupling.

Alternatively, four antennas are designed as a building block by decoupling all the adjacent two antennas [24] – [26]. In [24],

Manuscript received December 31, 2021; revised May 1, 2022, and June 14, 2022; accepted June 17, 2022. This work was supported in part by Science, Technology and Innovation Commission of Shenzhen Municipality under grant RCBS20210706092348050, and in part by Guangdong Basic and Applied Basic Research Foundation under grant 2021A1515110728. (*Corresponding author: Jiangwei Sui.*)

Jiangwei Sui and Cuixia Huang are with the School of Electronics and Communication Engineering, Sun Yat-sen University—Shenzhen Campus, Guangming, Shenzhen 518107, China (e-mail: suijw@mail.sysu.edu.cn; huangcx7@mail2.sysu.edu.cn).

Yi-Feng Cheng is with the School of Electronics and Information, Hangzhou Dianzi University, Hangzhou 310018, China (e-mail: chengyifeng2013@gmail.com).

four linearly-placed open-slot antennas are connected using three neutralization lines between the adjacent antennas. By properly tuning the width and length of the neutralization lines, the mutual coupling between the adjacent antennas can be reduced to below -12 dB. Three lumped elements are used to decouple the adjacent mutual couplings of a four-element inverted-F (IFA) antenna block in [25], with the outer two face-to-face IFA pairs decoupled using two inductors and the inner two back-to-back IFAs decoupled using a capacitor. In [26], four linearly-arranged open slot antennas are designed by decoupling the adjacent antenna elements. Although the adjacent mutual couplings are suppressed by using these methods, the non-adjacent antenna pairs are not decoupled resulting from the working mechanism limitations. According to the measurement study in [3], a lower mutual coupling means higher throughput, so the mutual couplings of the non-adjacent antenna pairs require to be further mitigated to obtain a much higher system throughput.

In this paper, a multi-element fully-decoupled linearly-placed IFA array is proposed for the 3.5 GHz (3.3 – 3.8GHz) band application in mobile terminals. Compared with the existing designs that only decouple the inner-pairs [17] – [23] or the adjacent pairs [24] – [26] in a four-element antenna block, the proposed decoupling approach decouples not only the adjacent but also the non-adjacent antenna pairs, achieving a fully-decoupled multi-element antenna array. To the best of the authors' knowledge, this is the first fully-decoupled multi-element antenna design for mobile terminal applications.

This paper is organized as follows: the decoupling scheme and the two-stage decoupling process are studied using a four-element IFA example in Section II; Section III presents the measured results of two examples, one four-element design and one eight-element design using two proposed four-element IFA blocks, and one six-element IFA linear array is also designed to prove the generality of the proposed method; finally, conclusions are given in Section IV.

II. Decoupling Scheme and Process

In this part, the decoupling scheme of the proposed fully-decoupled four-element IFAs is firstly presented, followed by the two-stage decoupling process.

A. Decoupling Scheme

Fig. 1 shows three different decoupling schemes for four-element MIMO antennas, where only two inner-pair antennas are decoupled [17] – [23] in Fig. 1(a) and three adjacent mutual couplings are addressed [24] – [26] in Fig. 1(b). And Fig. 1(c) depicts the proposed decoupling scheme, where all the six mutual couplings among the four IFAs, marked as IFA 1, IFA 2, IFA 3 and IFA 4, are mitigated, achieving fully-decoupled MIMO antennas. These six mutual couplings belong to six different antenna pairs, three back-to-back pairs (IFAs 1&2, IFAs 3&4, and IFAs 1&4), one face-to-face pair (IFAs 2&3), and two back-to-face pairs (IFAs 1&3 and IFAs 2&4) [14], [26]. Here 'back' denotes the short end direction and 'face' denotes the open end direction of the IFA. Taking the geometry symmetry into consideration, there are four mutual

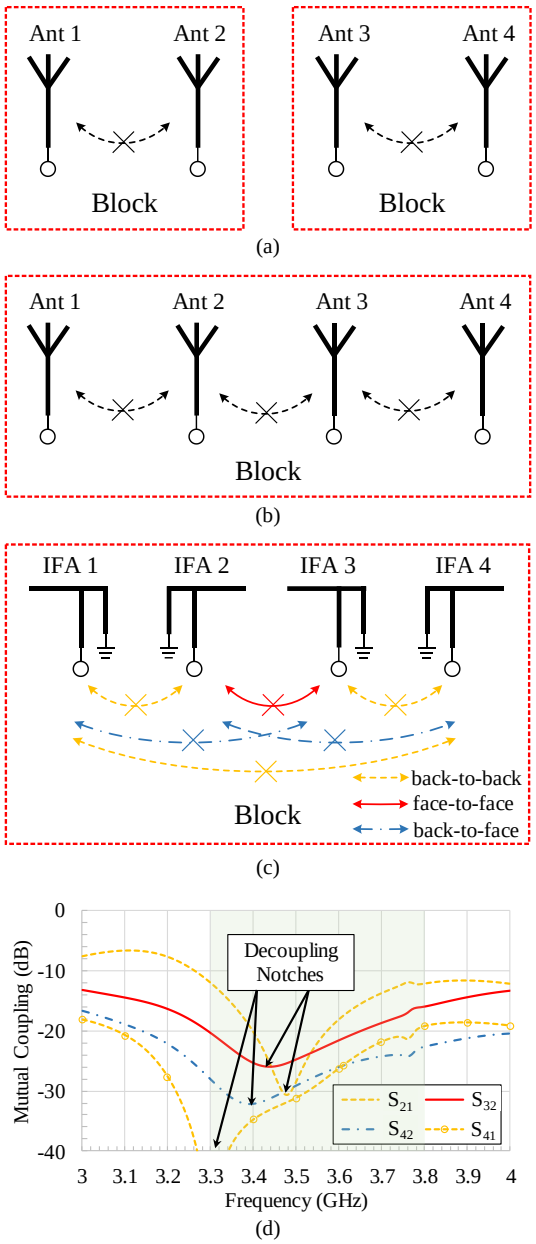

Fig. 1. Three different decoupling schemes for four-element MIMO antennas in mobile terminals. (a)Two couplings of inner-pair are mitigated in prior designs. (b) Three couplings of adjacent antenna pairs are mitigated in prior designs. (c). All the six couplings among the IFAs are mitigated in the proposed design. (d) Simulated couplings of the proposed four-element IFAs.

couplings to be dealt with, S_{21}, S_{32}, S_{42} and S_{41}. As shown in Fig. 1(d), there generates a decoupling notch for all these four mutual couplings, justifying the fully-decoupled characteristic of the proposed four-element IFAs.

Fig. 2 depicts the detailed geometry of the proposed four-element IFA array. The whole design imitates a typical mobile terminal, consisting of two PCB boards, a 150 × 75 mm horizontally-placed mainboard, and a vertically-placed sideboard of 7-mm height. Four IFAs working at 5G N78 band (3.3 – 3.8 GHz) are printed mirror-symmetrically on the outer side of the sideboard and top side of the mainboard. The mainboard is double-sided with the bottom side as the ground plane, and the four IFAs are connected with the ground plane

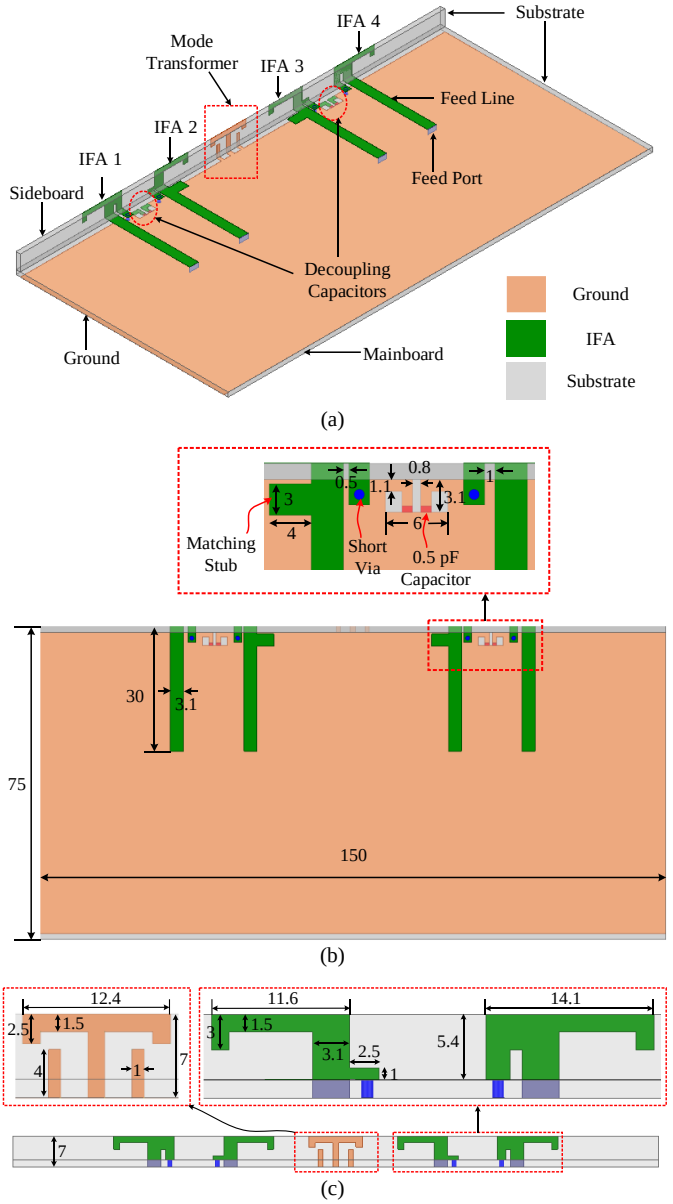

Fig. 2. Geometries of the proposed four-element fully-decoupled IFAs. (a) Perspective view. (b) Top view. (c) Side view. The unit used here is millimeter.

through four short pins, marked as blue circle dots in Fig. 2. The substrate used for the PCB boards is 1.6-mm thick FR4 with permittivity of 4.3 and loss tangent of 0.02.

As shown in Fig. 2(a), one pair of decoupling capacitors are inserted between IFA 1 and IFA 2 as well as IFA 3 and IFA 4, so that the two mutual couplings of the back-to-back IFA pairs, S_{21} (the same as S_{43}) and S_{41}, can be effectively suppressed. And for the remaining back-to-face and face-to-face pairs, a T-shaped decoupling radiator is introduced between the two face-to-face IFAs, IFA 2 and IFA 3. This decoupling radiator works as a mode transformer, transforming the original unbalanced IFA mode of IFA 2 into a balanced loop mode to confine the ground current and spatial field nearby the exciting antenna and mode transformer so that the couplings will not be induced on the original victim antennas, IFA 3 (face-to-face with IFA 2) and IFA 4 (back-to-face with IFA 2).

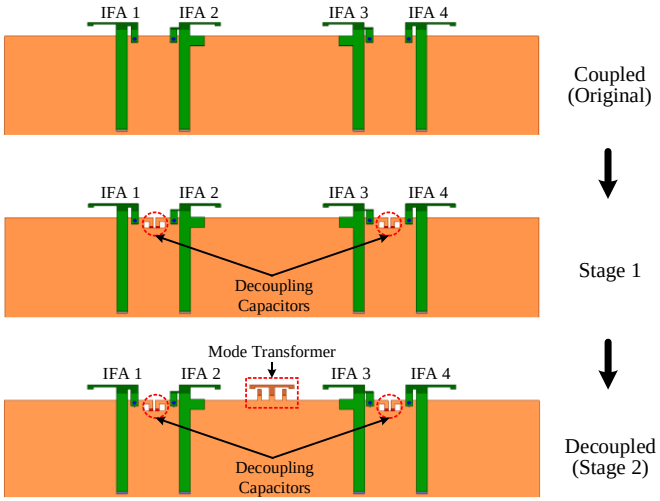

Fig. 3. Decoupling process of the proposed four-element fully-decoupled IFAs.

In summary, the decoupling process consists of two stages, as depicted in Fig. 3.

Stage 1: four decoupling capacitors are used to decouple the two back-to-back IFA pairs (IFAs 1&2, and IFAs 1&4), as is shown in Fig. 3(b);

Stage 2: a mode transformer is designed to decouple the face-to-face (IFA 2&3) and back-to-face (IFA 1&3) IFA pairs, as is presented in Fig. 3(c).

B. Stage 1: Decoupling of Back-to-Back IFA Pairs

First, two back-to-back IFA pairs are decoupled using the self-curing decoupling technique by adding four decoupling capacitors. Following the calculation process introduced in [14], two 0.5 pF capacitors are obtained and inserted between IFA 1 and IFA 2, as well as between IFA 3 and IFA 4, as is shown in Fig. 3(b). As the S-parameters compared in Fig. 4(a), there generates a decoupling notch for mutual couplings S_{21} and S_{41} of Stage 1, meaning that the two back-to-back cases are decoupled by introducing the decoupling capacitors. However, for the face-to-face IFA pair, as S_{32} shown in Fig. 4(b), after introducing the decoupling capacitor for dealing with S_{21} and S_{41}, the coupling level worsens to -7 dB at a certain frequency within the N78 band. This is understandable because no decoupling capacitor locates between the two concerned IFAs due to the capacitor loading position constraint [14], and this is the main limit of this decoupling capacitor method. Due to this constraint, this decoupling capacitor method cannot fully decouple a multi-element IFA array since there are three types of pairs in a linear array, back-to-back, back-to-face, and face-to-face, in which only back-to-back pairs can be well decoupled by introducing decoupling capacitors. And for S_{42}, only the decoupling capacitor loaded on IFA 4 locates between IFA 2 and IFA 4, which can perturb the mutual current effectively, and the other one behind IFA 2 works weakly, leading to not as good coupling reduction as S_{21} and S_{41}.

One thing that deserved to be discussed is the impedance bandwidth. Fig. 4(c) describes the comparison of matching conditions between the IFAs of the coupled case and Stage 1. It

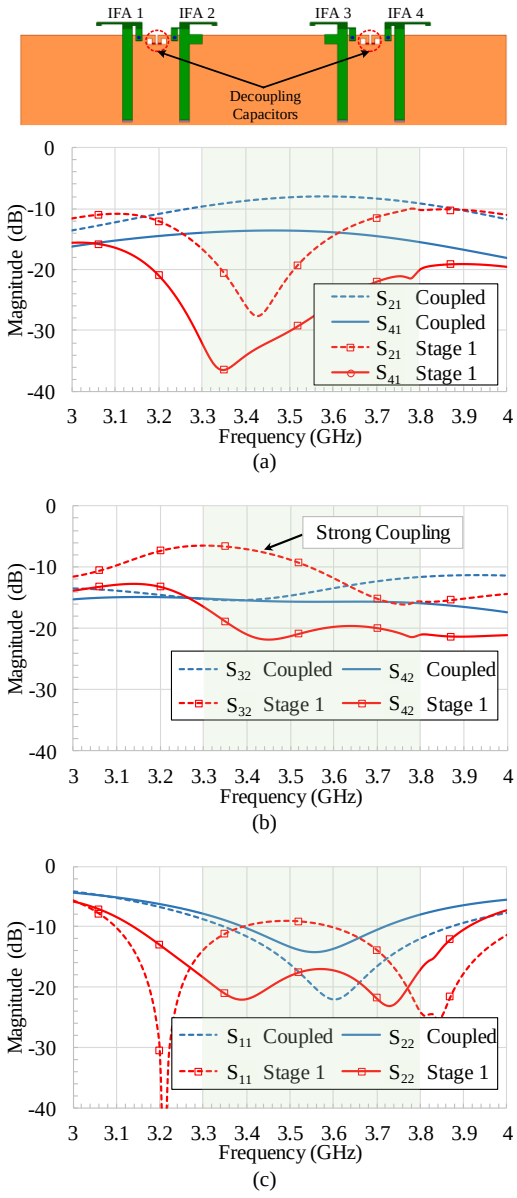

Fig. 4. Simulated S-parameters comparison of IFAs of coupled case and Stage 1. (a) S_{21} and S_{41}. (b) S_{32} and S_{42}. (c) S_{11} and S_{22}.

is seen that for Stage 1, the loaded decoupling capacitor transforms the single-resonance IFA into a dual-resonance one, effectively enhancing the matching bandwidth. The dual-resonance phenomenon by adding a capacitor can be explained using the transmission line models, as depicted for a dual-band IFA design [27].

C. Stage 2 (Decoupled): Decoupling of Face-to-Face and Back-to-Face IFA Pairs

In Stage 1, the two back-to-back IFA pairs (IFAs 1&2, IFAs 1&4) are decoupled by using the self-curing decoupling capacitors. However, the remaining face-to-face (IFAs 2&3) and back-to-face pairs (IFAs 2&4) are still not decoupled. This issue will be addressed in this Stage 2.

As the simulated current distribution of Stage 1 is shown in Fig. 5(a), when IFA 2 is fed, an IFA mode is excited, which is an unbalanced mode [22], meaning that the ground will also

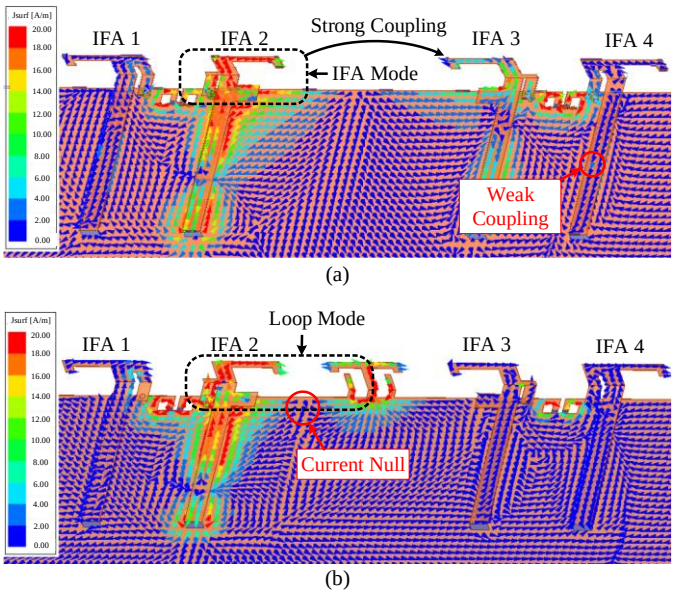

Fig. 5. Simulated current distributions of Stage 1 and Stage 2 when IFA 2 is excited. (a) Stage 1. (b) Stage 2.

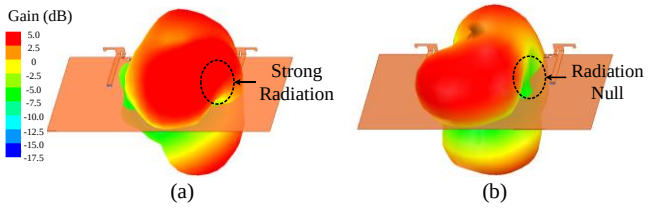

Fig. 6. Simulated radiation patterns of Stage 1 and Stage 2 when IFA 2 is excited. (a) Stage 1. (b) Stage 2.

radiate power to some extent by inducing somewhat current. Due to the strong electric-field induction [25] of the face-to-face case, IFA 3 will induce a strong coupling current. Besides, IFA 4 also induces a weak coupling from IFA 2 because IFA 4 is also located in the coupling area of IFA 2 due to their back-to-face configuration.

In this study, a mode transformer is proposed to transform the radiating mode of the active antenna, here setting IFA 2 as an example, so that IFA 3 and IFA 4 do not locate in the strong coupling area of IFA 2 anymore. Therefore, mutual couplings S_{32} and S_{42} can be mitigated simultaneously. It can be seen from the current distribution shown in Fig. 5(b) that the T-shaped mode transformer induces most of the coupling from IFA 2, constituting a loop mode together with IFA 2. Because this loop mode is balanced [22], most of the energy is constrained around IFA 2 and the mode transformer, leaving almost no coupling currents on IFA 3 and IFA 4.

To reveal the decoupling mechanism more clearly, the radiation patterns of Stage 1 and Stage 2 are compared in Fig. 6. In the simulations, IFA 2 is excited with the other ports are terminated with 50-Ω matched loads. For Stage 1, where there is no T-shaped mode transformer, some power radiates in the right direction, leading to a strong mutual coupling between IFA 2 and IFA 3, which has been justified from the strong S_{32} in Fig. 4(b) and strong coupling current from Fig. 5(a). After

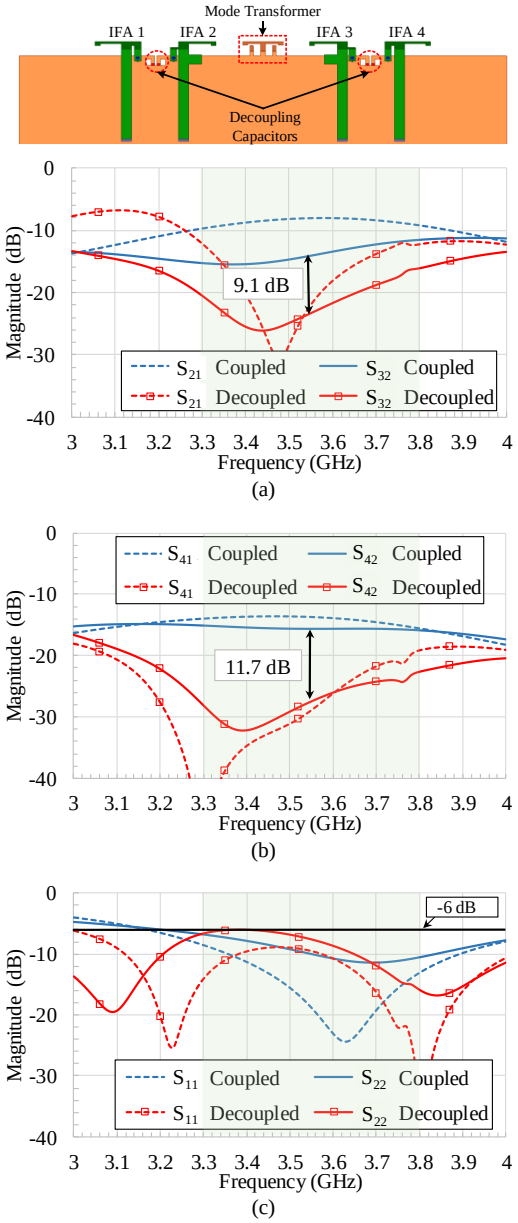

Fig. 7. Simulated S-parameters of coupled and decoupled (Stage 2) IFAs. (a) S_{21} and S_{32}. (b) S_{42} and S_{41}. (c) S_{11} and S_{22}.

introducing the T-shaped mode transformer, there generates a radiation null in the right part due to the balanced loop mode, as shown in Fig. 6(b), therefore mitigating the mutual coupling between IFA 2 and IFA 3 as well as IFA 2 and IFA 4.

The simulated S-parameters of the coupled antennas and the proposed decoupled antennas (Stage 2) are compared in Fig. 7. It is seen from Fig. 7(a) that, for the two kinds of adjacent mutual couplings, S_{21} and S_{32}, about 9 dB reduction is achieved throughout the N78 band. Simultaneously, the other two kinks of mutual couplings, S_{42} and S_{41}, are also reduced by about 11 dB in the whole N78 band, as is shown in Fig. 7(b). At this stage, all the four kinds of antenna pairs of the four-element IFAs are decoupled using the hybrid decoupling methods which consist of four decoupling capacitors and one mode transformer. Moreover, a wideband impedance matching is

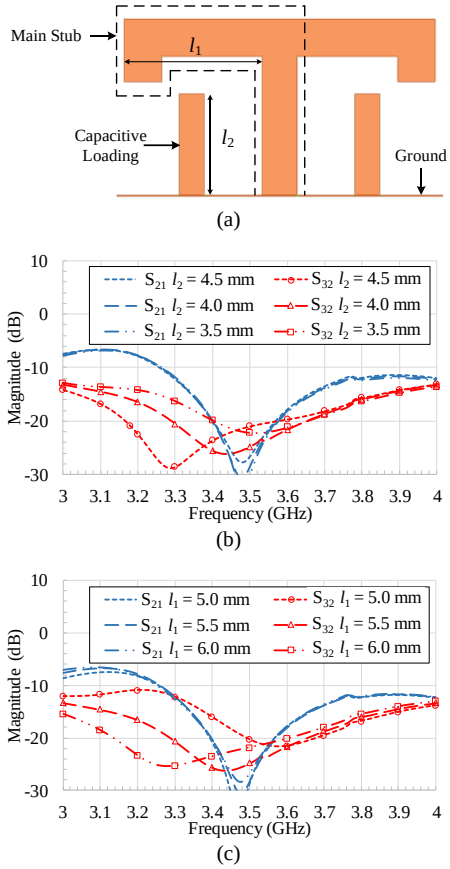

Fig. 8. Parametric study of the mode transformer. (a) Geometry of the mode transformer. (b) Study with l_2. (c) Study with l_1.

obtained by introducing two resonances using the loading capacitors, as is shown in Fig. 7(c).

D. Tuning Procedures

As shown in Fig. 8(a), there are two parts of the mode transformer, the main stub and the capacitive loading. The main stub works like a typical quarter-wavelength radiator, and the capacitive loading is added to decrease the resonant frequency of the whole radiator [28]. Besides, it is found that the capacitive loading helps achieve a better isolation level throughout the N78 band. When l_2 decreases, the capacitive coupling between the loading stub and the main stub also decreases, so the resonant frequency turns higher, leading to a higher decoupling frequency, as is shown in Fig. 8(b). Similarly, as shown in Fig. 8(c), when l_1 increases, the electrical length increases, so the resonant frequency and decoupling frequency turn lower. In both the studies of l_1 and l_2, it is seen that the S_{21} maintains almost the same, presenting a relatively independent tuning feature. In summary, when tuning the mode transformer, l_1 should be tuned to make the decoupling frequency located within the desired band, and then l_2 needs to be adjusted with l_1 to balance the decoupling frequency and decoupling level.

III. Demonstration Examples

A. Four-Element IFAs

The original coupled and proposed decoupled antennas discussed in Section II are fabricated and measured. It is seen

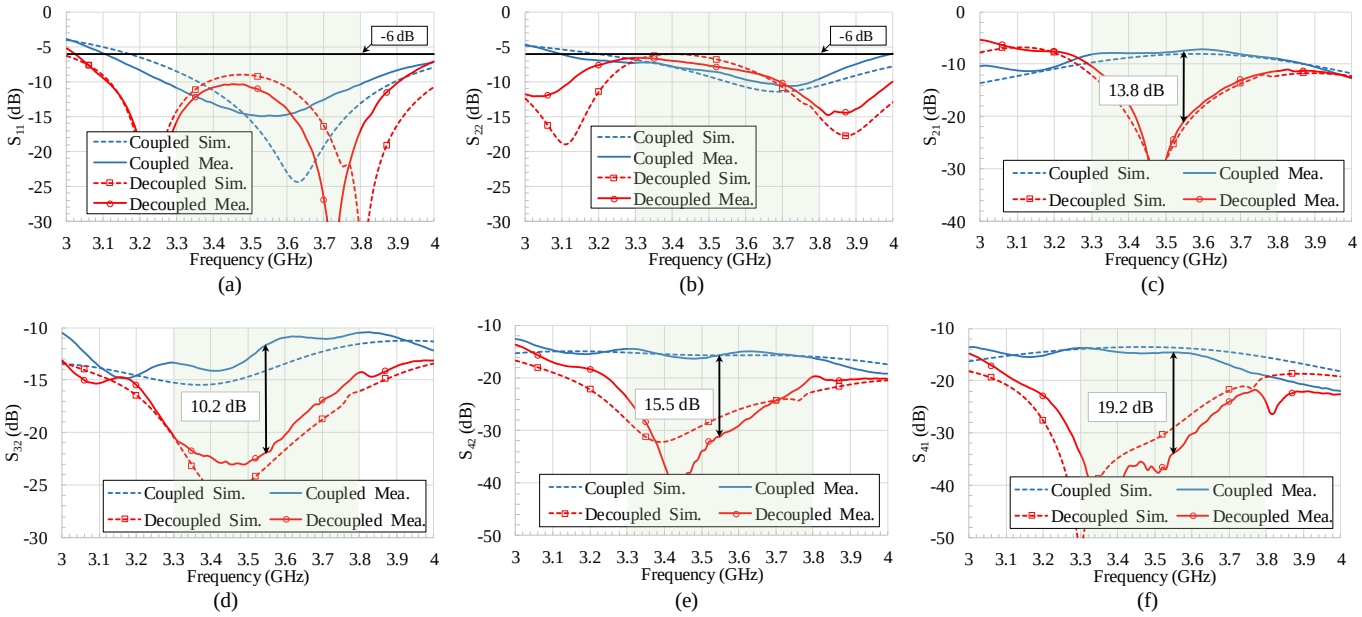

Fig. 9. Simulated and measured S-parameters of coupled and proposed decoupled antennas. (a) S_{11}. (b) S_{22}. (c) S_{21}. (d) S_{32}. (e) S_{42}. (f)S_{41}.

from Figs. 9 (a) and (b) that the matching condition is better than -6 dB in the whole N78 band. The two adjacent mutual couplings, S_{21} and S_{32}, are presented in Figs. 9 (c) and (d). After decoupling, S_{21} is lower than -12 dB and S_{32} is lower than -15 dB from 3.3 GHz to 3.8 GHz. If taking the narrower N78 band (3.4 – 3.6 GHz) as an application scenario, S_{21} is lower than -17.5 dB and S_{32} is lower than -20 dB in the whole band, showing a high isolation level for terminal phones. The other two mutual couplings, S_{42} and S_{41}, are compared in Figs. 9 (e) and (f), showing that the couplings are reduced by about 10 dB after decoupling, and the achieved coupling level is lower than -20 dB from 3.3 GHz to 3.8 GHz.

It is well-known that the most crucial parameter for terminal antennas is total efficiency, which is determined by radiation efficiency and S-parameters of the MIMO antennas as follows,

$$\eta_{Total,i} = (1-|S_{ii}|^2-\sum_{j\neq i}|S_{ij}|^2)\times\eta_{Radiation,i} \quad i=1,2 \qquad (1)$$

where $\eta_{total,i}$ and $\eta_{radiation,i}$ denote the total efficiency and radiation efficiency of i_{th} IFA, respectively, with S_{ii} and S_{ij} denoting the matching and mutual couplings of the IFAs, respectively. As formula (1) indicates, to achieve a high total efficiency after decoupling, the radiation efficiency should be high, and the reflection coefficiency and mutual couplings should be as low as possible.

The total efficiencies of the coupled and decoupled four-element IFAs are measured in an accredited near-field anechoic chamber, as the photo shown in Fig. 10. And the simulated and measured total efficiencies are compared in Fig. 11, where the simulated efficiencies are calculated using formula (1). It is found that the average total efficiency improves from 57 % to 72 % for IFA 1 (the same as IFA 4) after decoupling. And for IFA 2 (the same as IFA 3), the total efficiency of the decoupled one decreases slightly from 3.3 to 3.4 GHz compared with the coupled one, this is mainly because the reflection coefficient of IFA 2 is a litter higher and radiation

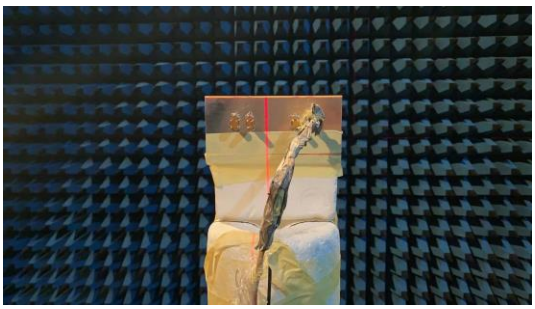

Fig. 10. A photo of total efficiency measurement of the prototyped four-element IFAs in an anechoic chamber.

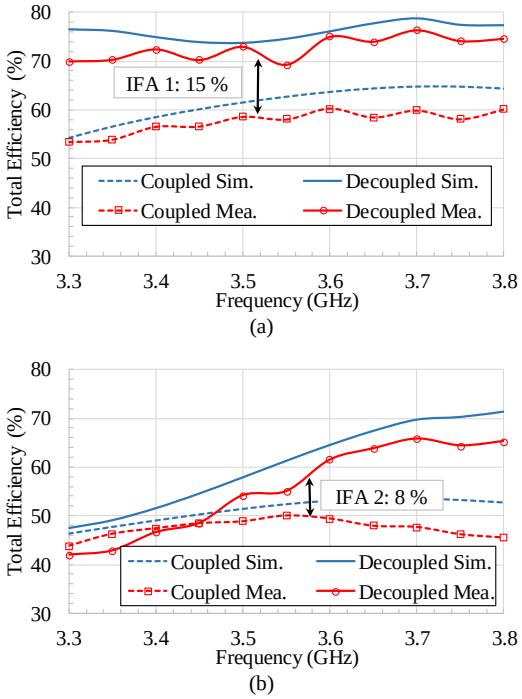

Fig. 11. Simulated and measured total efficiencies of the coupled and decoupled IFA 1 and IFA 2. (a) IFA 1. (b) IFA 2.

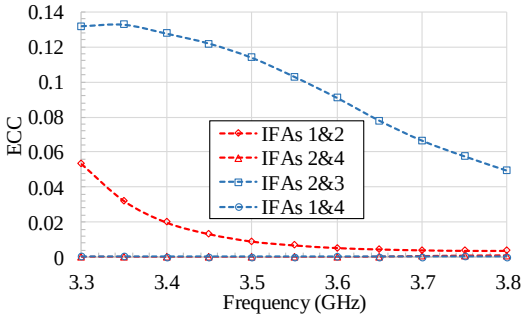

Fig. 12. Calculated ECCs using measured far fields of the proposed four-element fully-decoupled IFAs.

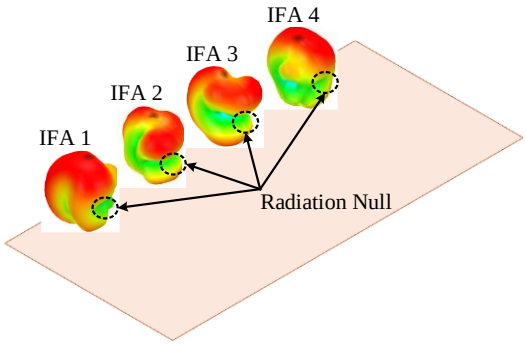

Fig. 13. Simulated radiation patterns of the proposed four-element fully-decoupled IFAs.

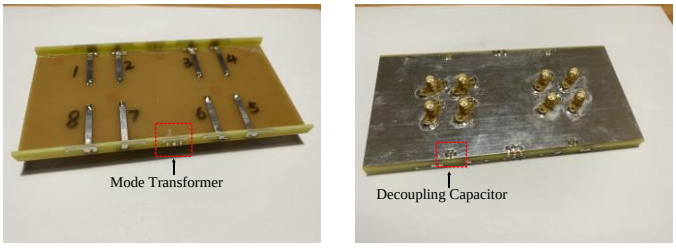

(a) (b)

Fig. 14. Figures of the proposed eight-element MIMO antennas. (a) Top side. (b) Bottom side.

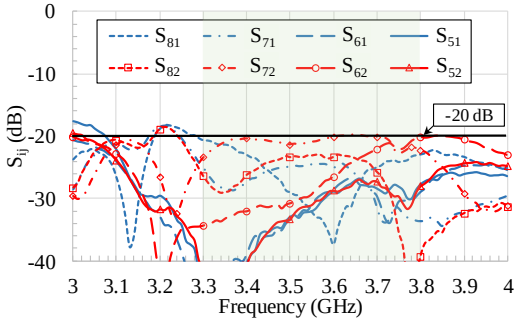

Fig. 15. Measured mutual couplings among the IFAs of different four-element blocks.

efficiency of IFA 2 becomes a litter lower after decoupling in the band from 3.3 to 3.4 GHz. However, in the whole N78 band from 3.3 to 3.8 GHz, the average total efficiency of IFA 2 still improves from 47 % to 55 %, justifying that the decoupled IFAs radiate more power into free space than the coupled ones.

Besides the S-parameters decoupling, the field-level spatial correlation decoupling is also characterized using envelope correlation coefficient (ECC) by studying the correlation of two antennas' far-field electric fields [29]. Fig. 12 presents the calculated ECCs of every pair of the proposed four-element IFAs using the measured far-field data. It is seen that for all the four kinds of antenna pairs, IFA 1 and IFA 2, IFA 2 and IFA 3, IFA 2 and IFA 4, and IFA 1 and IFA 4, the ECCs are all lower than 0.14, suggesting a good MIMO spatial performance.

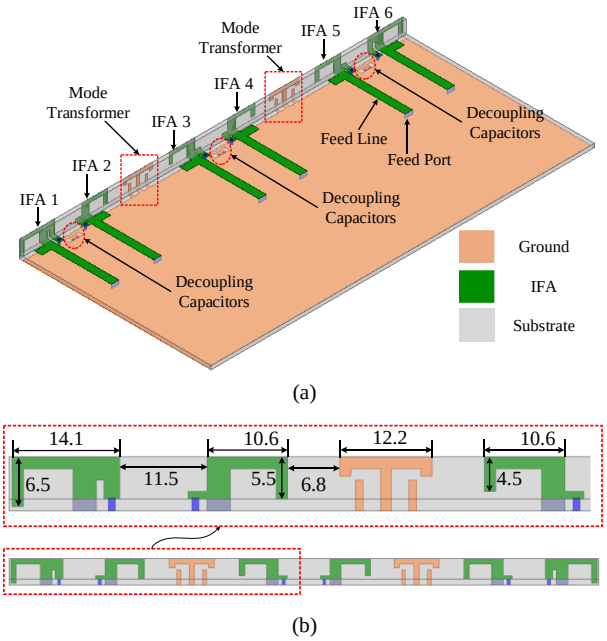

Fig. 16. Geometry of the six-element fully-decoupled IFAs. (a) Perspective view. (b) Side view.

B. Eight-Element IFAs

To provide a much higher data rate, eight-element MIMO antennas may be implemented in the mobile phone in the future, at least for some bands. Benefiting from the outside radiation, as is shown in Fig. 13, there is a radiation null towards another long-side of the main PCB board for all the four IFAs, indicating low mutual coupling in this direction. Therefore, in this part, another identical four-element IFA block is mirrored-symmetrically placed on the other side of the main PCB board, forming an eight-element MIMO antenna design.

Fig. 14 shows the prototype of the eight-element IFAs consisting of two proposed four-element building blocks. The measured mutual couplings between two IFAs across the two sides are presented in Fig. 15, which are all lower than -20 dB, justifying the prior pattern diversity analysis.

C. Six-Element IFAs

To justify the generality of the proposed hybrid decoupling method, a six-IFA MIMO design is studied in this part. To accommodate six IFAs, a larger main PCB board, 160 × 80 mm, is used. The geometry of the six-element IFAs is presented in Fig. 16(a), showing that three back-to-back pairs are arranged vertically on the sideboard. Taking into consideration the geometry symmetry, there are nine mutual couplings in total: 1) four back-to-back types, S_{21}, S_{43}, S_{41}, and S_{61}; 2) three back-to-face types, S_{31}, S_{51}, and S_{42}; and 3) two face-to-face

TABLE I

COMPARISON OF SOME HIGH-ORDER MIMO ANTENNAS FOR MOBILE TERMINALS

Ref.	Antenna Number in a Basic Block	Decoupling Number of Antenna Pairs*	-6 dB Bandwidth	Size of the Four-Element Antenna Unit (Length×Ground Clearance×Height)	Isolations	ECCs	Total Efficiency
[17][2017]	2	2	3.4 – 3.6 GHz	35×1×7 mm^3	> 10 dB	< 0.15	40 – 52 %
[19][2018]	2	2	3.4 – 3.6 GHz	12×1.8×7 mm^3 (Two-Element)	> 20 dB/ > 17 dB	< 0.07	49 – 56.4 % 61.6 – 72.9 %
[21][2019]	2	2	3.4 – 3.6 GHz	25×1.5×7 mm^3 (Two-Element)	> 20 dB/ >12.7 dB	< 0.13	29.2 – 54.1 %
[23][2020]	2	2	3.3 – 5 GHz	100×3×7.5 mm^3	> 21 dB/ > 12 dB	< 0.11	58.9 – 88.6 % 31.6 – 76.7 %
[24][2016]	4	3	3.4 – 3.6 GHz	50×3×0.8mm^3	> 12 dB	< 0.25	40 – 60 %
[25][2019]	4	3	3.4 – 3.6 GHz	38.2×0×3.2 mm^3	> 11.8 dB	N.A.	40 – 55 %
[26][2021]	4	3	3.3 – 5 GHz	60×2×6 mm^3	> 10 dB	< 0.3	40 – 75 %
Proposed	4	6	3.3 – 3.8 GHz/ 3.4 – 3.6GHz	103.2×1.6×7 mm^3	> 12 dB/ > 17.5 dB	< 0.14	IFA 1: 69 – 76 % IFA 2: 42 – 66%

*This parameter denotes the decoupling number of antenna pairs among four antennas.

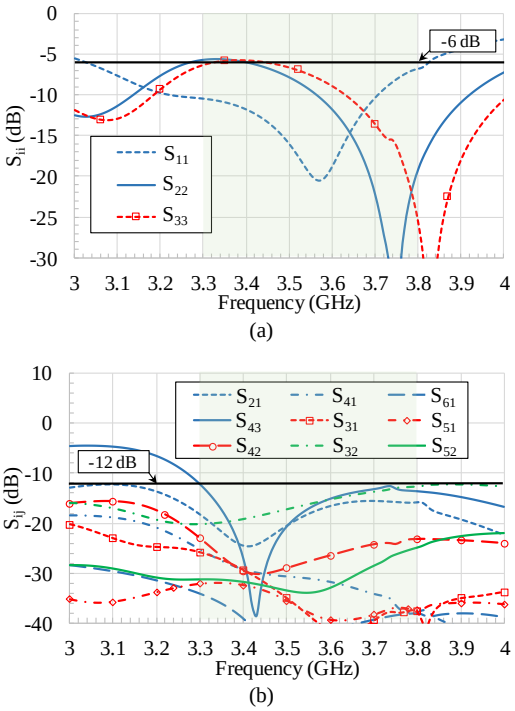

Fig. 17. Simulated S-parameters of the six-element fully-decoupled IFAs. (a) Matching conditions. (b) Mutual couplings.

types, S_{32} and S_{52}. Similar to the four-element IFAs, three groups of decoupling capacitors are inserted between the three adjacent back-to-back IFA pairs to mitigate the four back-to-back mutual couplings, and two mode transformers are introduced between the two adjacent face-to-face IFA pairs, IFAs 2 and 3 as well as IFAs 4 and 5, to address the three back-to-face and two face-to-face mutual couplings. Fig. 16(b) marks the antenna dimensions that are different from those in Fig. 2 for the four-element IFAs. As the simulated S-parameters show in Figs. 17(a) and (b), two resonances are generated by using the proposed method, and there is a decoupling notch for all the nine mutual couplings among the six-element IFAs, justifying that these six-element IFAs are fully-decoupled using the proposed hybrid decoupling method.

D. Comparison with Prior Works

In this part, the proposed four-element IFAs are compared with some prior high-order MIMO antennas in mobile terminals from several aspects, as is summarized in Table I. The design methods can be mainly divided into three kinds according to their antenna number in a basic block and decoupling numbers of antenna pairs among four antennas. First, as has been shown in Fig. 1(a), a decoupled antenna pair is designed as a basic unit [17] – [19], [21], [23], and two units are adopted to form a four-element MIMO antenna system. Second, a four-element block is designed as a basic unit [24] – [26], and three adjacent antenna pairs are decoupled but leaving the non-adjacent antenna pair alone, as has been shown in Fig. 1(b). Third, in this proposed design, all the mutual couplings between every two IFAs in the four-element IFA block are decoupled, not only for the three adjacent IFA pairs but also for the three non-adjacent IFA pairs, as has been justified in Fig. 10. And compared with other four-element block designs, the other performances of the proposed design, such as -6 dB bandwidth, antenna size, isolation, ECC, and total efficiency, are all

TABLE II

COMPARISON OF SOME T-SHAPED DECOUPLING STRUCTURES

Ref.	Decoupling Structure	Co-Design with Antennas	Decoupling Number of Antenna Pairs
[30][2012]	T-shaped ground branch	No	1
[31][2014]	T-shaped parasitic element	No	1
[32][2012]	T-shaped slot	No	1
[33][2014]	Two Inverted-L branches + slot	No	1
Proposed	T-shaped mode transformer	Yes	3 / 9

competitive. One point should be mentioned is that the total efficiency of IFA 2 is a little lower than that of IFA 1 after decoupling, and this is because the matching condition and radiation efficiency of IFA 2 in the lower band (about 3.3 – 3.4 GHz) is a little poorer than those in the higher band for both the coupled and decoupled scenarios. However, when compared with the coupled IFAs, the total efficiencies of both the IFA 1 and IFA 2 are improved after decoupling, as can be seen from Fig. 11, justifying the effectiveness of the proposed method.

And another comparison is about the T-shaped decoupling structures. As shown in Table II, a T-shaped ground branch [30], [31], a T-shaped slot [32], and a combination of branches and slot [33] can be used to decouple two antennas by introducing another coupling path from the T-shaped structure to cancel out with the original coupling. And the used T-shaped structure is an independent component, whose design does not require considering the antennas' orientation and current mode since it only requires introducing another coupling path. Different from these designs, there are multiple antenna pairs required to be addressed in a multi-element design, and the traditional T-shaped structure functioning through coupling cancellation cannot address all these multiple pairs due to the freedom limitation. In the proposed method, the T-shaped structure is co-designed with the coupled IFAs, which is unique from the existing two-element designs. The T-shaped structure is introduced into a face-to-face IFA pair so that the excited IFA and the corresponding half of the T-shaped structure will form a loop structure, which is a balanced mode. Therefore, the ground current will be confined nearby the excited IFA and the T-shaped structure, preventing the coupling induced on the original victim IFAs, IFA 3 (face-to-face pair with IFA 2) and IFA 4 (back-to-face pair with IFA 2), as is shown in Fig. 5(b). Different from the coupling cancellation function of the T-shaped structure in the existing designs, the T-shaped structure functions as a mode transformer, transforming the original unbalanced IFA mode into the balanced loop mode, so that not only the face-to-face pairs but also the non-adjacent back-to-face pairs can be decoupled.

IV. CONCLUSION

A multi-element fully-decoupled IFA block is proposed in this paper. All the mutual couplings among the antennas are mitigated using a hybrid decoupling method, which introduces multiple decoupling capacitors and decoupling radiators. In addition to decoupling the back-to-back IFA pairs, the decoupling capacitors also enhance the impedance bandwidth of each IFA by generating two resonances. The decoupling radiator works as a mode transformer, turning the IFA element from an unbalanced IFA mode into a balanced loop mode, preventing the mutual current from spreading to the victim antennas of the face-to-face and back-to-face IFA pairs. One four-element IFA array using the proposed decoupling method is designed and measured. The measured results show that after decoupling, all the six mutual couplings are reduced by about 10 dB throughout the N78 band (3.3 – 3.8 GHz), and the average total efficiency improves from 57 % to 72 % for IFA 1, and from 47 % to 55 % for IFA 2, as well as with all the ECCs lower than 0.14. Another eight-element IFA array is designed based on the pattern diversity of two proposed four-element IFA blocks, showing inter-block isolation better than 20 dB and similar inner-block isolation as the first four-element example. Moreover, a six-element linear IFA array is also designed to justify the generality of the proposed decoupling method.

ACKNOWLEDGMENT

The authors would like to express their deep appreciation to Prof. Ke-Li Wu at The Chinese University of Hong Kong for his valuable and inspirational discussion and suggestions, and to Mr. Yun-Ming Leo Fung there for his kind help with antenna efficiency measurement. Many thanks also go to the concerned Editors and Reviewers for their valuable and constructive comments.

REFERENCES

[1] WRC-15 Press Release. (Nov. 27, 2015). World Radiocommunication Conference Allocates Spectrum for Future Innovation. [Online]. http://www.itu.int/net/pressoffice/press_releases/2015/56.aspx

[2] M. A. Jensen and J. W. Wallace, "A review of antennas and propagation for MIMO wireless communications," *IEEE Trans. Antennas Propag.*, vol. 52, no. 11, pp. 2810–2824, Nov. 2004.

[3] X. Mei and K.-L. Wu, "How low does mutual coupling need to be for MIMO antennas," in *Proc. IEEE Antennas Propag. Soc. Int. Symp.*, Boston, MA, USA, Jul. 2018, pp. 1579–1580.

[4] A. Diallo, C. Luxey, P. L. Thuc, R. Staraj, and G. Kossiavas, "Study and reduction of the mutual coupling between two mobile phone PIFAs operating in the DCS1800 and UMTS bands," *IEEE Trans. Antennas Propag.*, vol. 54, no. 11, pp. 3063–3073, Nov. 2006.

[5] I. Dioum, A. Diallo, S. M. Farssi, and C. Luxey, "A novel compact dual-band LTE antenna-system for MIMO operation," *IEEE Trans Antennas Propag.*, vol. 62, no. 4, pp. 2291–2296, Apr. 2014.

[6] S.-C. Chen, Y.-S. Wang, and S.-J. Chung, "A decoupling technique for increasing the port isolation between two strongly coupled antennas," *IEEE Trans. Antennas Propag.*, vol. 56, no. 12, pp. 3650–3658, Dec. 2008.

[7] Y.-F. Cheng and K.-K. M. Cheng, "A novel dual-band decoupling and matching technique for asymmetric antenna arrays," *IEEE Trans. Microw. Theory Techn.*, vol. 66, no. 5, pp. 2080–2089, May. 2018.

[8] X. Zhao, S. P. Yeo, and L. C. Ong, "Decoupling of inverted-F antennas with high-order modes of ground plane for 5G mobile MIMO platform," *IEEE Trans. Antennas Propag.*, vol. 66, no. 9, pp. 4485–4495, Sep. 2018.

[9] H. Li, Z. Miers, and B. K. Lau, "Design of orthogonal MIMO handset antennas based on characteristic mode manipulation at frequency bands below 1 GHZ," *IEEE Trans. Antennas Propag.*, vol. 62, no. 5, pp. 2756–2766, May. 2014.
[10] B. K. Lau and J. B. Andersen, "Simple and efficient decoupling of compact arrays with parasitic scatterers," *IEEE Trans. Antennas Propag.*, vol. 60, no. 2, pp. 464–472, Feb. 2012.
[11] H. Xu, H. Zhou, S. Gao, H. Y. Wang, and Y. J. Cheng, "Multimode decoupling technique with independent tuning characteristic for mobile terminals," *IEEE Trans. Antennas Propag.*, vol. 65, no. 12, pp. 6739-6751, Dec. 2017.
[12] J. Sui and K.-L. Wu, "A self-decoupled antenna array using inductive and capacitive couplings cancellation," *IEEE Trans. Antennas Propag.*, vol. 68, no. 7, pp. 5289-5296, Jul. 2020.
[13] S. Zhang, B. K. Lau, Y. Tan, Z. Ying, and S. He, "Mutual coupling reduction of two PIFAs with a T-shape slot impedance transformer for MIMO mobile terminals," *IEEE Trans. Antennas Propag.*, vol. 60, no. 3, pp. 1521–1531, Mar. 2012.
[14] J. Sui, Y. Dou, X. Mei, and K.-L. Wu, "Self-curing decoupling technique for MIMO antenna arrays in mobile terminals," *IEEE Trans. Antennas Propag.*, vol. 68, no. 2, pp. 838-849, Feb. 2020.
[15] M.-Y. Li et al., "Eight-port orthogonally dual-polarized antenna array for 5G smartphone applications," *IEEE Trans. Antennas Propag.*, vol. 64, no. 9, pp. 3820–3830, Sep. 2016.
[16] Y. Li, C.-Y.-D. Sim, Y. Luo, and G. Yang, "High-isolation 3.5 GHz eight-antenna MIMO array using balanced open-slot antenna element for 5G smartphones," *IEEE Trans. Antennas Propag.*, vol. 67, no. 6, pp. 3820–3830, Jun. 2019.
[17] K.-L. Wong, C.-Y. Tsai, and J.-Y. Lu, "Two asymmetrically mirrored gap-coupled loop antennas as a compact building block for eight-antenna MIMO array in the future smartphone," *IEEE Trans. Antennas Propag.*, vol. 65, no. 4, pp. 1765–1778, Apr. 2017.
[18] Z. Ren, A. Zhao, and S. Wu, "MIMO antenna with compact decoupled antenna pairs for 5G mobile terminals," *IEEE Antennas Wireless Propag. Lett.*, vol. 18, no. 7, pp. 1367–1371, Jul. 2019.
[19] L. Sun, H. Feng, Y. Li, and Z. Zhang, "Compact 5G MIMO mobile phone antennas with tightly arranged orthogonal-mode pairs," *IEEE Trans. Antennas Propag.*, vol. 66, no. 11, pp. 6364–6369, Nov. 2018.
[20] H. Xu, S. S. Gao, H. Zhou, H. Wang, and Y. Cheng, "A highly integrated MIMO antenna unit: Differential/common mode design," *IEEE Trans. Antennas Propag.*, vol. 67, no. 11, pp. 6724–6734, Nov. 2019.
[21] L. Chang, Y. Yu, K. Wei, and H. Wang, "Polarization-orthogonal co-frequency dual antenna pair suitable for 5G MIMO smartphone with metallic bezels," *IEEE Trans. Antennas Propag.*, vol. 67, no. 8, pp. 5212–5220, Aug. 2019.
[22] L. Chang, Y. Yu, K. Wei, and H. Wang, "Orthogonally polarized dual antenna pair with high isolation and balanced high performance for 5G MIMO smartphone," *IEEE Trans. Antennas Propag.*, vol. 68, no. 5, pp. 3487–3495, May 2020.
[23] L. Sun, Y. Li, Z. Zhang, and Z. Feng, "Wideband 5G MIMO antenna with integrated orthogonal-mode dual-antenna pairs for metal-rimmed smartphones," *IEEE Trans. Antennas Propag.*, vol. 68, no. 4, pp. 2494–2503, Apr. 2020.
[24] K.-L. Wong, J.-Y. Lu, L.-Y. Chen, W.-Y. Li, and Y.-L. Ban, "8-antenna and 16-antenna arrays using the quad-antenna linear array as a building block for the 3.5-GHz LTE MIMO operation in the smartphone," *Microw. Opt. Technol. Lett.*, vol. 58, no. 1, pp. 174–181, Jan. 2016.
[25] C. Deng, D. Liu, and X. Lv, "Tightly arranged four-element MIMO antennas for 5G mobile terminals," *IEEE Trans. Antennas Propag.*, vol. 67, no. 10, pp. 6353–6361, Oct. 2019.
[26] L. Sun, Y. Li, and Z. Zhang, "Wideband integrated quad-element MIMO antennas based on complementary antenna pairs for 5G smartphones," *IEEE Trans. Antennas Propag.*, vol. 69, no. 8, pp. 4466–4474, Aug. 2021.
[27] J. Sui and K.-L. Wu, "A capacitive loading method for turning a single-band antenna into dual-band for wireless terminal applications," *IEEE Antennas Wireless Propag. Lett.*, vol. 17, no. 12, pp. 2474-2478, Dec. 2018.
[28] C. R. Rowell and R. D. Murch, "A compact PIFA suitable for dual-frequency 900/1800-MHz operation," *IEEE Trans. Antennas Propag.*, vol. 46, no. 4, pp. 596–598, April 1998.
[29] R. G. Vaughan and J. B. Andersen, "Antenna diversity in mobile communications," *IEEE Trans. Veh. Technol.*, vol. VT-36, no. 4, pp. 147–172, Nov. 1987.
[30] C. Yang, Y. Yao, J. Yu, and X. Chen, "Novel compact multiband MIMO antenna for mobile terminal," *Int. J. Antennas Propag.*, vol. 2012, pp. 691681:1–691681:9, 2012.
[31] A. Toktas and A. Akdagli, "Wideband MIMO antenna with enhanced isolation for LTE, WiMAX and WLAN mobile handsets," *Electron. Lett.*, vol. 50, no. 10, pp. 723–724, 2014.
[32] S. Zhang, B. K. Lau, Y. Tan, Z. Ying, and S. He, "Mutual coupling reduction of two PIFAs with a T-shape slot impedance transformer for MIMO mobile terminals," *IEEE Trans. Antennas Propag.*, vol. 60, no. 3, pp. 1521–1531, Mar. 2012.
[33] S. Shoaib, I. Shoaib, N. Shoaib, X. Chen, and C. G. Parini, "Design and performance study of a dual-element multiband printed monopole antenna array for MIMO terminals," *IEEE Antennas Wireless Propag. Lett.*, vol. 13, pp. 329–332, 2014.

Jiangwei Sui received the B.S. degree from University of Science and Technology of China, Hefei, China, in 2014, and the Ph.D. degree from The Chinese University of Hong Kong, Hong Kong, China, in 2019. From 2019 to 2020, he was with vivo Mobile Communication Co., Ltd. as an antenna engineer. Since 2021, he has been an Assistant Professor with the School of Electronics and Communication Engineering, Sun Yat-sen University. His current research interests include antenna array decoupling techniques and associated MIMO antenna design for wireless communication applications.

Cuixia Huang received the B.S. degree in communication engineering from Sun Yat-sen University, Guangzhou, China, in 2021, where she is now pursuing the M.S. degree. Her current research interests include 5G terminal antenna design and antenna array decoupling techniques.

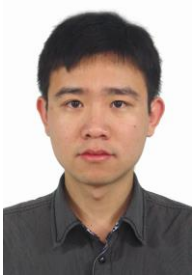

Yi-Feng Cheng received the B.Eng. degree from the University of Electronic Science and Technology of China, Chengdu, China, in 2014, and the Ph.D. degree from The Chinese University of Hong Kong, Hong Kong, in 2020, where he was a Postdoctoral Fellow from 2020 to 2021. Since 2021, he has been an Associate Research Fellow with the School of Electronics and Information, Hangzhou Dianzi University. His current research interests include microwave theory, antenna theory, RF circuit design, and MIMO antenna decoupling techniques.